

**Low TCD and High Velocity SAW Devices Based on AlN/diamond structure**

**M. El Hakiki<sup>+</sup>, O. Elmazria<sup>+</sup>, V. Mortet<sup>#</sup>, M.B. Assouar<sup>+</sup>, L. Bouvot<sup>+</sup>, M. Nesladek<sup>\*</sup>, and P. Alnot<sup>+</sup>.**

<sup>+</sup>LPMIA – UMR 7040, Université H. Poincaré - Nancy I – F-54506, France.

<sup>#</sup>Institute of Physics, Academy of Sciences of the Czech Republic, , Czech Republic.

<sup>\*</sup>IMO – Limburgs Universitair Centrum – B-3590 Diepenbeek, Belgium.

Mohamed.Elhakiki@lpmi.uhp-nancy.fr

**Abstract**

Feasibility of fabricating AlN/diamond SAW devices on unpolished nucleation side of freestanding CVD diamond have been demonstrated. We have shown experimentally that this structure shows a very good combination of high velocity, high electromechanical coupling coefficient ( $K^2$ ) and low TCD. We have observed that the TCD decreases when AlN thickness increases confirming that AlN and diamond exhibit intrinsic TCD values with opposite signs. Realization of SAW filters with zero TCD on AlN/diamond structure is then possible without using an additional layer such as SiO<sub>2</sub>. Curves of phase velocity and electromechanical coupling coefficient as a function of the normalized thickness of AlN was determined by simulation and compared to experimental ones showing a good agreement. However, TCD values of this structure calculated for various AlN thickness and various propagation modes show a strange divergence with experiments. This divergence is probably due to the unavailability of precise temperature coefficient of the elastic constants.

**Introduction**

Thanks to its unequalled high acoustic velocity, CVD diamond combined with piezoelectric film as Aluminium nitride (AlN) shows an attractive solution for the development of GHz-band surface acoustic wave (SAW) devices [1]. The AlN/diamond structure have been fabricated by sputtering c-axis oriented aluminium nitride films on unpolished nucleation side of freestanding polycrystalline CVD diamond. The nucleation side, obtained after silicon substrate etching, shows a smooth surface and no polishing is required. Details concerning the technological process and deposition parameters were elsewhere [2-3].

In the work reported in this paper, we have studied the SAW characteristics in IDTs/AlN/diamond structure by theoretical calculation and experiments. We have calculated the dispersive curves of normalized of phase velocity, electromechanical coupling coefficient ( $K^2$ ) and the temperature coefficient of delay TCD, of the IDT/AlN/Diamond structure. Results obtained by simulation will be compared to experimental ones.

**Theoretical analysis**

The general equations describing the SAW propagation in a piezoelectric medium are governed by [4-5] :

$$C_{ijkl} \frac{\partial^2 U_l}{\partial x_j \partial x_k} + e_{kij} \frac{\partial^2 \Phi}{\partial x_j \partial x_k} = \rho \frac{\partial^2 U_i}{\partial t^2} \quad (1)$$

$$e_{jkl} \frac{\partial^2 U_l}{\partial x_j \partial x_k} - \epsilon_{jks}^s \frac{\partial^2 \Phi}{\partial x_j \partial x_k} = 0 \quad (2)$$

where  $\rho$ ,  $C_{ijkl}$ ,  $e_{ijkl}$ ,  $\epsilon_{ijkl}$  are respectively the mass density, elastic, piezoelectric and dielectric tensors of the considered material.  $U$  is the particle displacement and  $\phi$  the scalar electric potential. The coordinate system is depicted in figure 1.  $X_1$  is the propagation direction.

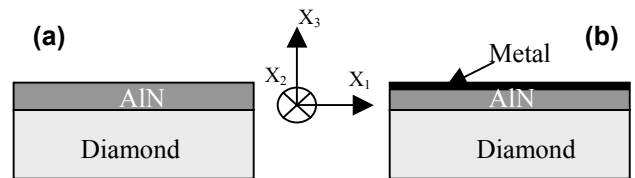


**Figure1:** Schematics of AlN/diamond structure  
**(a)** Open circuit and **(b)** Short circuit

The particle displacement and the potential in each medium are assumed to be a linear combination of the partial waves expressed as:

$$U_l = A_l \exp(-jkbx_3) \exp[jk(vt - x_1)] \quad (3)$$

$$\phi = A_4 \exp(-jkbx_3) \exp[jk(vt - x_1)] \quad (4)$$

with  $l = 1, 2, 3$

When (3) and (4) are substituted in (1) and (2), the eighth-order equation for  $b$  is obtained in each medium. Usually  $b$  is taken as a complex number, and the imaginary part of  $b$  must be negative in the substrate because the wave amplitude should evanesce in the  $-X_3$  direction in the substrate. Since the field component of Rayleigh waves must exponentially

decay into the substrate. Only four decay coefficients with negative imaginary parts are used for the substrate. Thus there are four partial waves in the substrate and eight in the layer. For instance, in the case of AlN/diamond structure, the general solution for the displacement and the potential satisfying (1) and (2) are given as:

$$U_i^{Dia} = \sum_{n=1}^4 C_n^{Dia} A_i^{Dia(n)} \exp(-jkb_{Dia}^{(n)}x_3) \exp[jk(vt - x_1)] \quad (5)$$

$$\phi^{Dia} = \sum_{n=1}^4 C_n^{Dia} A_4^{Dia(n)} \exp(-jkb_{Dia}^{(n)}x_3) \exp[jk(vt - x_1)] \quad (6)$$

$$U_i^{AlN} = \sum_{n=1}^8 C_n^{AlN} A_i^{AlN(n)} \exp(-jkb_{AlN}^{(n)}x_3) \exp[jk(vt - x_1)] \quad (7)$$

$$\phi^{AlN} = \sum_{n=1}^8 C_n^{AlN} A_i^{AlN(n)} \exp(-jkb_{AlN}^{(n)}x_3) \exp[jk(vt - x_1)] \quad (8)$$

By substituting equations (5) to (8) into the following boundary conditions:

$$U_i^{Dia} = U_i^{AlN}, T_{i3}^{Dia} = T_{i3}^{AlN}, D_i^{Dia} = D_i^{AlN}, \phi^{Dia} = \phi^{AlN}$$

We can obtain the following form:

$$[G] [C_1^{Dia} C_2^{Dia} C_3^{Dia} C_4^{Dia} C_1^{AlN} \dots C_8^{AlN}]^t = 0 \quad (9)$$

where G is a  $12 \times 12$  matrix.

The condition that the matrix  $[C_1^{Dia} C_2^{Dia} C_3^{Dia} C_4^{Dia} C_1^{AlN} \dots C_8^{AlN}]^t$  has the solution except zero matrix gives the following relation:  $\text{Det}(G) = 0$  and phase velocity  $V$  is derived from this condition.

The values of electromechanical coupling coefficient  $K^2$  were determined analytically by using the relation:

$$K^2 = 2 \frac{V_f - V_s}{V_f} \quad (10)$$

where  $V_f$  and  $V_s$  are the theoretical SAW velocities determined as described above when the plane of the constant  $X_3$ , where the IDT is located, is electrically open and short circuited, respectively (figure 1).

The theoretical temperature coefficient of delay is obtained by the next relation [6]:

$$TCD = \alpha \frac{v(35^\circ) - v(15^\circ)}{20 \cdot v(25^\circ)} \quad (11)$$

where  $v(35^\circ)$ ,  $v(15^\circ)$ ,  $v(25^\circ)$ , are phase velocities at  $35^\circ\text{C}$ ,  $15^\circ\text{C}$ ,  $25^\circ\text{C}$ , respectively, and  $\alpha$  is the thermal

expansion coefficient along the SAW propagation direction. The material constants and temperature coefficient of stiffness constants used in the calculation are listed in table 1 and 2 respectively [6-7].

**Table 1:** Material constants used in the calculation

		AlN	Diamond
Elastic Constants ( $\times 10^{11} \text{N/m}^2$ )	$C_{11}$	3.45	10.8
	$C_{12}$	1.25	1.25
	$C_{13}$	1.20	1.25
	$C_{33}$	3.95	10.8
	$C_{44}$	1.18	5.76
Piezoelectric constants ( $\text{C/m}^2$ )	$e_{15}$	-0.48	-----
	$e_{31}$	-0.58	-----
	$e_{33}$	1.5	-----
Relative dielectric constants ( $\times 10^{-11} \text{F/m}$ )	$\epsilon_{11}$	8	5.7
	$\epsilon_{33}$	9.5	5.7
Masse density ( $\times 10^3 \text{Kg/m}^3$ )	$\rho$	3.26	3.51

**Table 2:** Temperature coefficient of Material Constants used in the calculation

		AlN	Diamond
Temperature Coefficients of Elastic constants $\times 10^{-4}$	$(1/C_{11})(dC_{11}/dT)$	0.8	-0.14
	$(1/C_{12})(dC_{12}/dT)$	1.8	-0.57
	$(1/C_{13})(dC_{13}/dT)$	1.6	-0.57
	$(1/C_{33})(dC_{33}/dT)$	1	-0.14
	$(1/C_{44})(dC_{44}/dT)$	0.5	-0.125
Temperature Coefficients of Masse density $\times 10^{-6}$	$(1/\rho)(d\rho/dT)$	-14.6	-3.6

## Results and discussion

### 1- Phase velocity

Phase velocity dispersion curves obtained by calculation and a compilation of experimental points are shown in figure 3. The x axis represents the normalized thickness of AlN film ( $kh_{AlN}$ ), where  $k$  is the wave vector and  $h_{AlN}$  the thickness of AlN film.

The experimental points reported in Fig. 3, were obtained by frequency characterization of SAW filters using a network analyzer (HP8752A) and using the relation:  $V = f_0 \cdot \lambda$ .

where  $f_0$  is the center frequency of filter and  $\lambda$  is the spatial period of IDT. We can observe that experimental points fit very well with theoretical prediction for mode 0, 1, and 2. This indicates that the synthesized layers (AlN and diamond) exhibits the same elastic constants as those of single crystals used to perform the simulation.

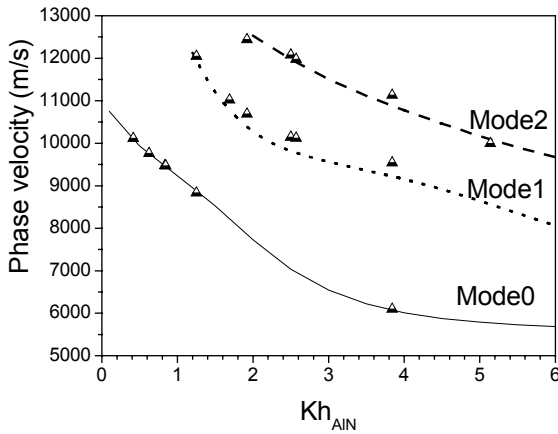


**Figure 3:** . Phase velocity dispersion curves of AlN/diamond structure. compilation of experimental results (symbol) and calculation (solid line).

2- Electromechanical coupling coefficient ( $K^2$ )

The dispersion curves of the coupling coefficient for IDT/AlN/diamond are shown in Figure 4. For the IDT/AlN/diamond configuration, the higher  $K^2$  values (1.37%) are obtained for the 1<sup>st</sup> mode wave. The small dependence of  $K^2$  on AlN thickness in the range [ $kh_{AlN} = 2$  to 4] is highly suitable for manufacturing. The experimental values of  $K^2$  was obtained by measuring the transducer's radiation resistance  $R_a$ , statistic capacitance  $C_s$  and resonance frequency  $f_0$  of response ( $S_{11}$ ).  $K^2$  was calculated from the following relation.

$$K^2 = \pi^2 / 2 \cdot f_0 \cdot C_s \cdot R_a \quad (11)$$

Figure 5 shows experimental values of  $K^2$  of IDT/AlN/diamond structure, obtained for the mode 1 versus the AlN normalized thickness. We can observe that measured values are two times higher than those predicted by calculation. More details concerning explanations in relation with these discrepancies have been presented elsewhere [3],[8].

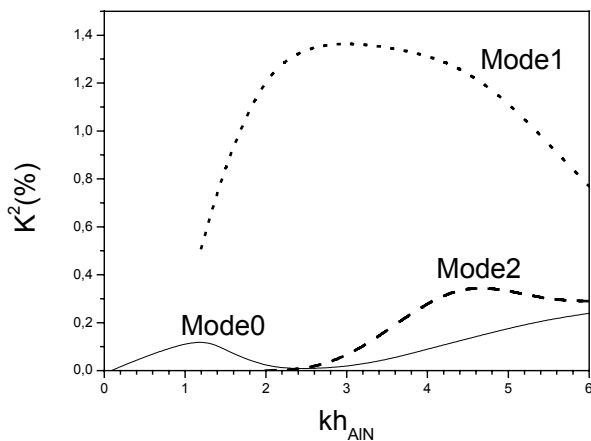


**Figure 4:** Dispersion curves for coupling coefficient of IDT/AlN/diamond structure.

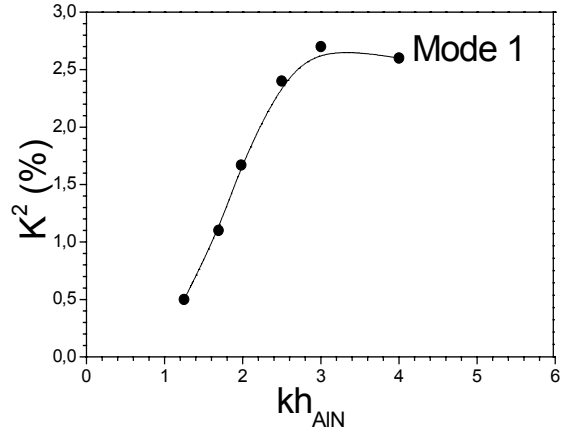


**Figure 5:**  $kh_{AlN}$  dependences of  $K^2$  measured from the IDT/AlN/diamond structure for the mode 1.

3- Temperature coefficient of delay (TCD)

The calculated  $kh_{AlN}$  dependence of TCD for the AlN/diamond is shown in figure 6-a. One can observe that the TCD value of mode 0 changes the sign and the zero TCD is obtained for  $kh_{AlN} = 0.36$ . Concerning the modes 1 and 2, TCD is negative in all the studied range [ $kh_{AlN} = 1.2$  to 6].

The experimental temperature coefficient of delay was determined by using the following relationship:

$$TCD = -\frac{1}{f_0} \times \frac{\Delta f}{\Delta T} \quad (12)$$

where  $f_0$  is the center frequency of SAW and  $\Delta f$ , the frequency shift corresponding to  $\Delta T$  variation.

The  $kh_{AlN}$  dependence of TCD measured for the IDT/AlN/diamond structure is shown in figure 6-b. We can notice that the three modes exhibit positive TCD values i for the range of used  $kh_{AlN}$  values. One can notice the big discrepancy existing in between theoretical and experimental results, although the different curves decrease in a similar manner. This fact can be explained by errors made in the calculation due to errors made on the determination temperature coefficients of elastic constants of AlN film [6][9]. Others experimental methods used for the determination of these constants, for AlN and CVD diamond layers are in progress in our laboratory. Brillouin spectroscopy is thought to be a good technique for this determination. The establishment of precise simulation leads to the determination by calculation of the required AlN thickness for zero TCD AlN/diamond structure.

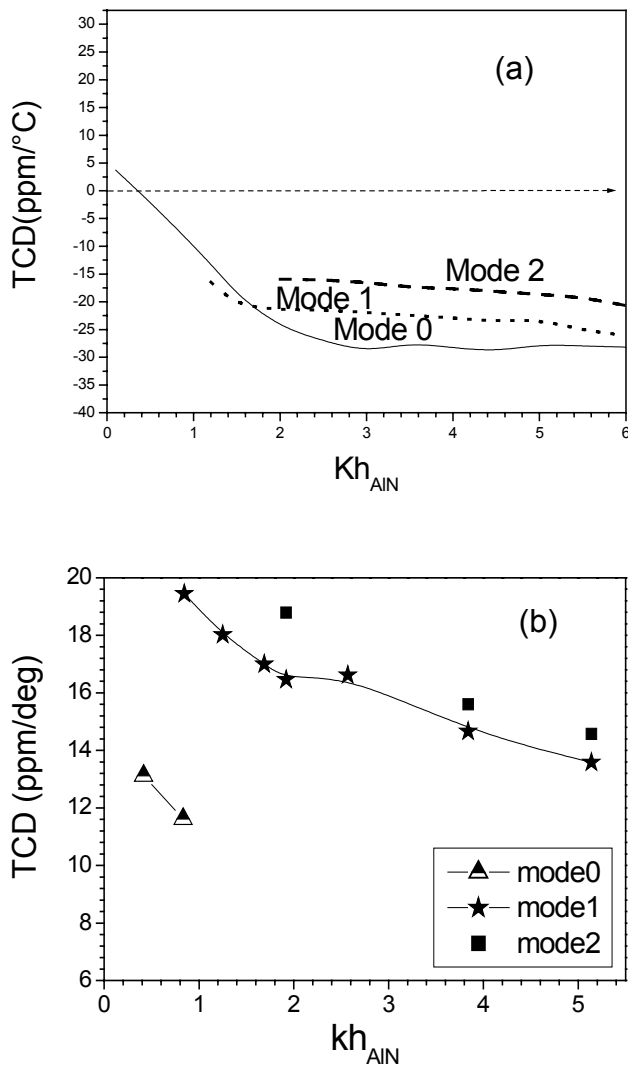


**Figure 6:** Calculated (a) and measured (b)  $kh_{AIN}$  dependences of TCD in IDT/AIN/diamond structure for modes 0, 1 and 2.

### Conclusion

In this paper, SAW devices based on AIN/diamond structure. have been characterized and results were compared to simulation. Experimental results demonstrate that these materials are very promising for fabrication of SAW devices operating at high frequency. Moreover high electromechanical coupling coefficient and a low temperature coefficient of Delay were experimentally found. Curves of phase velocity and electromechanical coupling obtained by calculation are in good agreement with experimental measurements. However, the calculated TCD values are not at all in agreement with experimental ones.

This discrepancy was related to the difference in between real temperature coefficients of elastic constants of our layers and the ones in our calculation, obtained from literature [6][9].

### References

- [1] S.-I. Shikata. Low-Pressure Synthetic Diamond. Eds.: B. Dischler and C. Wild. Springer-verlag Berlin Heidelberg 1998.
- [2] V. Mortet, O. Elmazria, M. Nesladek, M.B. Assouar, G. Vanhoyland, J. D'Haen, M. D'Olieslaeger, and P. Alnot. "Surface acoustic wave propagation in aluminium nitride-unpolished freestanding diamond structures"; Appl. Phys. Lett. Vol. 81, (2002) 1720.
- [3] O. Elmazria V. Mortet, M. El hakiki, M. Nesladek, and P. Alnot, "High velocity SAW Using Aluminium Nitride Film on Unpolished Nucleation Side of Free-Standing CVD Diamond" IEEE Trans. Ultrason., Ferroelect., Freq. Contr., Vol 50 N° 6, (2003) pp 710-715.
- [4] J. J. Campbell and W. R. Jones 'A method for estimating optical crystal cuts and propagation directions for excitation of piezoelectric surface waves.' IEEE Ultrasonics Symp., vol. 15, (1968) 209.
- [5] H. Nakahata, K. Higaki, S. Fujii, A. Hachigo, H.Kitabayashi, K. Tanabe, Y. Seki and S. Shikata "SAW Devices on Diamond", proc. 1995 IEEE Ultrasonics Symp., vol. 1, (1995) 361-370.
- [6] K.Tsubouchi, K.Sugai and N.Mikoshiba "Zero temperature coefficient surface acoustic wave devices using epitaxial AIN Films" Ultrasonics Symposium (1982) 340-345
- [7] A. J .Slobodinic, Jr., E. D. Conway, an R. T. Delmonico " Surface acoustic wave velocity, " in Microwave Acoustic Handbook, vol 1A. Air force Cambridge Research laboratory, Bedford, Ma, no. TR-73-0597, 1973.
- [8] T-T. Wu, and Y.-Y. Chen, "Exact Analysis of Dispersive SAW Devices on ZnO/Diamond/Si-Layered Structures" IEEE Trans. Ultrason.,Ferroelect., Freq. Contr., 49-1, (2002) 142-149,
- [9] K. Tsubouchi, N. Mikoshiba "Zero temperature coefficient SAW on AIN epitaxial Films" Ultrasonics Symposium (1985) 634-644.